Perspective: Chain dynamics of unfolded and intrinsically disordered proteins from nanosecond fluorescence correlation spectroscopy combined with single-molecule FRET

Benjamin Schuler
Department of Biochemistry and Department of Physics, University of Zurich, Winterthurerstrasse 190, Zurich, Switzerland

(Received 26 April 2018; accepted 18 June 2018; published online 3 July 2018)

The dynamics of unfolded proteins are important both for the process of protein folding and for the behavior of intrinsically disordered proteins. However, methods for investigating the global chain dynamics of these structurally diverse systems have been limited. A versatile experimental approach is single-molecule spectroscopy in combination with Förster resonance energy transfer and nanosecond fluorescence correlation spectroscopy. The concepts of polymer physics offer a powerful framework both for interpreting the results and for understanding and classifying the properties of unfolded and intrinsically disordered proteins. This information on long-range chain dynamics can be complemented with spectroscopic techniques that probe different length scales and time scales, and integration of these results greatly benefits from recent advances in molecular simulations. This increasing convergence between the experiment, theory, and simulation is thus starting to enable an increasingly detailed view of the dynamics of disordered proteins. *Published by AIP Publishing.*
https://doi.org/10.1063/1.5037683

PROTEIN STRUCTURE: FROM ORDER TO DISORDER

Proteins are the most versatile and functionally important components of living systems. This versatility is based on their heteropolymeric nature: a repertoire of 20 amino acids with chemically diverse side chains is used to generate proteins with very different structural and functional properties. Our notion of proteins has been shaped by the tremendous success of structural biology, which, ever since the crystal structure of myoglobin was solved some 60 years ago,[1] has revealed a stunning inventory of molecular machinery at atomic detail, ranging from globular enzymes soluble in aqueous solution and membrane proteins embedded in the hydrophobic environment of lipid bilayers to proteins that further assemble into higher order complexes or fibrous structures with unrivalled materials properties.

There is another side of the coin, however, which has been more difficult to access at the same level of detail—the properties of proteins when they do not assume such a well-folded three-dimensional structure that is amenable to crystallization. Such unfolded proteins are of great interest for at least two reasons. First, they constitute the starting point of the protein folding process, i.e., the transition of the polypeptide chain from the largely unstructured ensemble of configurations (e.g., after its synthesis on the ribosome) to the folded structure associated with its specific biological function. Over the past 20 years, however, a second important reason for investigating unfolded proteins has emerged: Based on a combination of biophysical experiments and bioinformatics, it has become evident that a large fraction of naturally occurring proteins are in fact unstructured under physiological conditions or contain long segments that are not folded, especially in higher organisms and viruses. According to current estimates, the fraction of such intrinsically disordered proteins (IDPs) in humans is greater than a third of all proteins.[2] Some IDPs retain an ability to fold, e.g., upon specific binding of a small molecule, a segment of DNA, or another protein.[3] Other IDPs, however, retain disorder even when bound to another protein.[4] It has thus become increasingly clear that IDPs are of functional importance for many biological processes, for instance, in cellular signal processing, gene regulation, or assembly of large complexes.[5]

These findings have stimulated a surging interest in the properties of unfolded and intrinsically disordered proteins and triggered three important developments: (i) advances in techniques that allow the dynamics of polypeptide chains to be studied experimentally;[6] (ii) the optimization of molecular dynamics (MD) force fields for atomistic simulations of these systems;[7–12] and (iii) a revival of polymer physics applied to protein configurations and dynamics.[13–18] In the context of protein folding, such measurements were motivated, in particular, by the search for a "speed limit" for structure formation,[19–21] ultimately given by the diffusive rate of contact formation within the chain. Correspondingly, triplet-state quenching techniques were employed that essentially require van der Waals contact between two groups in the polypeptide.[22,23] Closely related are fluorescence quenching techniques where complex formation between a fluorophore and a quencher in the chain causes photo-induced electron transfer, which results in fluctuations in emission that can be quantified by fluorescence correlation spectroscopy (FCS).[24–26] If the quenching efficiency and its distance dependence are sufficiently well known, the resulting rates of contact formation can be related to intramolecular distance distributions and an

effective diffusion coefficient between the chromophore and quencher.[27,28] However, characterizing the distance distribution usually requires independent information, and the analysis is very sensitive to the detailed shape of the distribution in the contact region.[29–31]

PROBING DISTANCES AND DISTANCE DISTRIBUTIONS IN UNFOLDED PROTEINS

An alternative approach that can provide access to both distance distributions and dynamics is Förster resonance energy transfer (FRET), which relies on the near-field dipole-dipole interactions between two fluorophores.[32] One fluorophore, the donor, absorbs a photon of incident light; the resulting excited-state energy can then be transferred to the other dye, the acceptor, in a nonradiative process. According to Förster's theory,[32] the rate of this energy transfer, k_T, varies with the distance between the donor and acceptor, r, as $k_T = k_D\,(R_0/r)^6$, where k_D is the fluorescence decay rate of the donor in the absence of an acceptor. The Förster radius, R_0, can be calculated from independently measurable spectroscopic quantities and characterizes the regime in which FRET is most sensitive to distance changes, typically between about 2 and 10 nm (depending on the Förster radius of the dye pair, which is typically between 5 and 7 nm), an ideal range for probing biological macromolecules. For a single fixed distance, the efficiency of energy transfer is defined in terms of the rate coefficients as $E = k_T/(k_T + k_D)$ and can thus be related to the distance via $E(r) = 1/\left(1 + r^6/R_0^6\right)$. In practice, E is most commonly determined by measuring either the transfer rate via the change in fluorescence lifetimes of the donor and/or acceptor or via the photon emission rates of the donor and acceptor, n_D and n_A, respectively, as $E = n_A/(n_A + n_D)$.[33]

FRET had been used to study biomolecules since the 1950s,[34] but a major breakthrough that led to a surge of activity in the field was its use in combination with single-molecule spectroscopy.[35] For protein folding studies, the use of confocal detection has been the dominant method, owing to its compatibility with time-correlated single-photon counting and the resulting high time resolution.[36,37] A key advantage of the single-molecule approach for studying protein folding and the properties of unfolded proteins is that it enables subpopulation-specific analyses. For example, in the case of a protein under conditions where only a fraction of the molecules is unfolded, the signal from the unfolded subpopulation can be analyzed selectively,[38–40] without interference from the signal of folded molecules (Fig. 1). (Note, however, that the rapid exchange between subpopulations during the time of diffusion through the confocal volume for proteins that fold in the sub-millisecond range can lead to time averaging in transfer efficiency histograms;[41] in this case, a more detailed analysis of the photon statistics or fluorescence lifetimes may be necessary.[42–46]) Another potential advantage is that very low (picomolar) concentrations of labeled proteins are required for single-molecule experiments, which can eliminate unwanted protein-protein interactions or protein aggregation, otherwise common for denatured proteins. Finally, owing to the fluorescence labeling, the properties of unfolded proteins can be investigated even in heterogeneous environments, be it in the presence of large concentrations of solutes to change solution conditions[47,48] or macromolecules to mimic crowding,[49] other components of the cellular machinery,[50,51] or even within live cells.[52]

The price for introducing fluorescence labels is that their interference with the macromolecular properties under investigation needs to be tested in every case, e.g., by comparing properties that are measurable with and without fluorophores [such as protein stability, biochemical activity, affinity to a binding partner, or comparisons to other spectroscopic methods, such as circular dichroism, nuclear magnetic resonance (NMR), etc.]; by determining fluorescence polarization anisotropies to verify dye mobility[45] (which indicates a lack of attractive interactions with the protein); or by placing the labels at different positions in the protein and comparing the results for consistency.[53,54] The Förster radii of currently available single-molecule FRET pairs allow investigations of unstructured polypeptides (or segments within larger proteins) between about 30 and 200 amino acids in length[18] (depending on their degree of expansion). For distances much less or much greater than the Förster radius, the sensitivity of the technique for distance changes decreases, and for very short distances, other processes (such as electron transfer) can compete with FRET, and the point-dipole approximation in Förster's theory may break down, preventing quantitative analysis.[55]

The most well-known application of single-molecule FRET is to obtain distance information on the molecular scale. In structured biomolecules, the observed transfer efficiency can be interpreted approximately in terms of a single distance, but unfolded and intrinsically disordered proteins sample exceedingly broad distributions of distances, $P(r)$. As a result, the contribution of all these distances must be taken into account for the average observed transfer efficiency[18,56]

$$\langle E\rangle = \int P(r)E(r)dr$$

(with the appropriate integration limits and normalization of the probability density function). Measurements in which the relevant observation time scale is much slower than the dynamics of the chain provide only this average value and no direct information about the shape of the distance distribution. This is the case, e.g., if transfer efficiency histograms are generated from the numbers of donor and acceptor photons from fluorescence bursts emitted by single unfolded protein molecules diffusing through the confocal volume [Fig. 1(b)]. Since the average interphoton time (microseconds) is much greater than the distance relaxation time within the chain (tens of nanoseconds, as explained below), the widths of the resulting transfer efficiency peaks are dominated by shot noise.[57] We thus need to assume a functional form for $P(r)$, which can, e.g., be approximated by simple polymer models or based on molecular simulations.[18] Since $E(r)$ is known (given the Förster radius), the measured $\langle E\rangle$ can be used to parameterize the distance distribution, if $P(r)$ is defined by a single adjustable parameter,[14,18] such as the mean-squared end-to-end distance for a Gaussian chain,[39] the persistence length for a worm-like chain,[58] or the scaling exponent or end-to-end distance for a

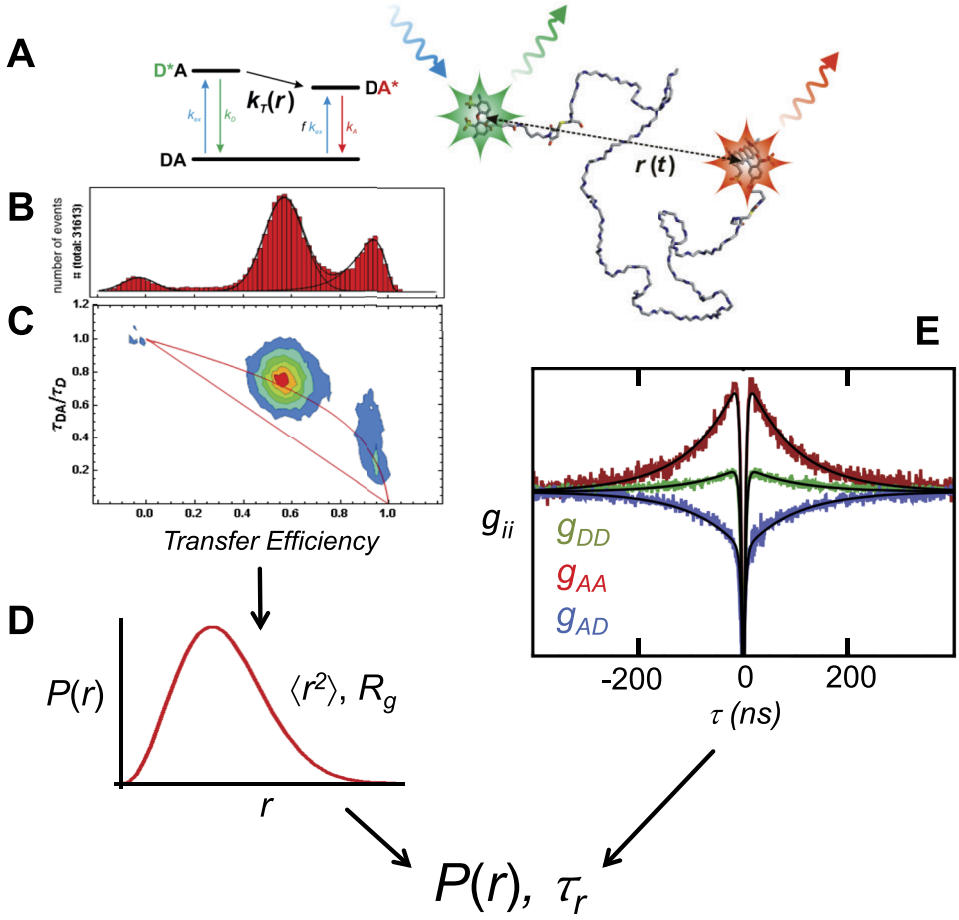

FIG. 1. Combining single-molecule FRET efficiency measurements with nanosecond correlation spectroscopy for quantifying distance distributions and dynamics in IDPs and unfolded proteins. (a) Illustration of an unfolded protein labeled with donor and acceptor fluorophores with a fluctuating intramolecular distance, $r(t)$, and a simple photophysical scheme representing the FRET process with the rate coefficients of the transitions. (b) Example of a transfer efficiency histogram illustrating the separation of an unfolded and a folded population (here at transfer efficiencies of ~0.6 and ~0.9, respectively), a key prerequisite for distinguishing changes in intramolecular distances in the unfolded state from those caused by folding. The small population at $E \approx 0$ is caused by molecules with a bleached, inactive, or absent acceptor fluorophore. (c) 2D histogram of relative fluorescence lifetime of the donor versus transfer efficiency. The straight line is the dependence expected for a fixed intramolecular distance,[45] and the curved line is the dependence expected for a broad distance distribution, here approximated by a Gaussian chain.[47] (d) The combined analysis of transfer efficiencies and fluorescence lifetime distributions can be used to quantify intramolecular distances in terms of a distance distribution characterized, e.g., by the mean squared end-to-end distance, $\langle r^2 \rangle$, or the radius of gyration, R_g. (e) Examples of nanosecond FCS measurements showing the donor (DD, correlated) and acceptor (AA, correlated) autocorrelations and the donor-acceptor (AD, anticorrelated) cross correlations with a decay on the ~100 ns time scale characteristic of the long-range dynamics in many unfolded proteins and IDPs.[40,47,69,70] The pronounced anticorrelated component below ~10 ns is caused by photon antibunching on the time scale of the fluorescence lifetime.[80] A global analysis of correlation functions, transfer efficiencies, and lifetimes can be used to quantify intramolecular distance distributions, $P(r)$, and chain reconfiguration times, τ_r, of IDPs and unfolded proteins. Adapted with permission from Brucale *et al.*, Chem. Rev. **114**(6), 3281–3317 (2014). Copyright 2014 American Chemical Society.[81]

suitably chosen self-avoiding walk[59] (the latter is arguably the most accurate of these simple models currently available).

Conversely, measurements in which the relevant observation time scale is shorter than the dynamics of the chain can provide additional information about the shape of the distance distribution. In typical single-molecule FRET experiments on unfolded proteins, this is the case for fluorescence lifetime measurements, which are available if confocal detection is combined with pulsed excitation and time-correlated single-photon counting.[45,60] The fluorescence lifetime (a few nanoseconds) is much shorter than the distance relaxation time within the chain, and so the decay of the fluorescence emission intensity, $I(t)$, depends on the shape of the distance distribution,

$$I(t) = I_0 \int_0^\infty P(r) e^{-t/\tau_{DA}(r)} dr,$$

where the mean donor fluorescence lifetime in the presence of the acceptor for a fixed distance is given by $\tau_{DA}(r) = \tau_D(1-E(r))$, and $\tau_D = 1/k_D$ is the donor lifetime in the absence of the acceptor. In principle, the shape of the distance distribution can thus be obtained from fluorescence lifetime measurements.[56] In practice, extracting the detailed shape of $P(r)$ is limited by the experimentally available signal-to-noise ratio, but lifetime information can yield a reliable measure of the variance of the underlying distance distribution.[42,43] As a result, the presence of a broad $P(r)$ yields a characteristic signature in plots relating transfer efficiencies quantified from the numbers of donor and acceptor photons to fluorescence lifetimes [Fig. 1(c)]: The deviation of the unfolded subpopulation from the diagonal line expected for a static population[44] is related to the variance of the underlying transfer efficiency (and thus distance) distribution.[18,42,43,47]

SINGLE-MOLECULE FRET OF PROTEIN DYNAMICS

Already in the 1970s, it was realized that the fluorescence lifetime decays of short peptides labeled with a FRET donor and acceptor contained information not only about the distance distribution but also about the dynamics of the chain if the fluorescence lifetime is in a similar range as the distance relaxation time.[61] Shortly after, in the context of the early developments of FCS,[62,63] the use of correlations between fluorescence photons in a FRET-labeled system was suggested theoretically as a way of extending this approach to dynamics of larger systems with dynamics slower than the typical fluorescence lifetimes of a few nanoseconds.[64] First indications that biopolymer dynamics can indeed result in detectable deviations from Poissonian photon statistics were reported in Hanbury Brown and Twiss-type[65,66] correlation experiments on DNA in 2002[67] and shortly after in simulations on peptides.[68] A few years later, rapid correlation experiments were first used for determining the dynamics of unfolded proteins.[40,69] Essentially, the distance fluctuations between the donor and acceptor fluorophore attached to specific positions in the chain lead to time correlations in photon emission. The loss of these correlations, reflected in the decay of the fluorescence intensity correlation function, can be related to the reconfiguration time of the chain, i.e., the relaxation time of the distance correlation function[40,68,70] [Fig. 1(e)]. This advance was facilitated by the previous decade of rapid developments in single-molecule FRET[35] for investigating biomolecules,[45,71] especially protein folding and dynamics,[72,73] including the theoretical methods for the quantitative analysis of photon statistics.[74,75] By monitoring FRET-labeled molecules individually, ensemble averaging is prevented, and so equilibrium fluctuations out of reach with ensemble methods became amenable to experimental investigation.

The information on chain dynamics is accessible with multi-channel confocal fluorescence detection combined with single-photon counting:[76] by distributing the photons onto two donor and two acceptor detectors and cross correlating the signal between them, the ~100 ns dead time of the avalanche photodiodes can be avoided,[65] and both the donor and acceptor autocorrelations and the donor-acceptor cross correlation are available from a single measurement (Fig. 1). A key strength of FRET is the combination of this information on the dynamics with the information on the intramolecular distance distributions:[18] From a joint analysis of the photon statistics of all three correlation functions (which exhibit the same relaxation time caused by chain dynamics) and the distance distribution parametrized based on transfer efficiency and fluorescence lifetimes, the properties of unfolded proteins can be quantified both in terms of their intramolecular distance distributions and their long-range dynamics (Fig. 1).[47,60,69] By placing the fluorophores into different positions within the chain, these properties can be mapped across different parts of the molecule to test for the consistency with simple polymer models or deviations that might be caused by heterogeneity in intrachain interactions.[47,53,54,77–79] In summary, single-molecule FRET in combination with rapid correlation analysis [nanosecond-FCS (nsFCS)] enables us to quantify both equilibrium distance distributions and chain dynamics in unfolded and intrinsically disordered proteins. These quantities provide a direct link to the concepts of polymer physics as a way of describing and understanding the behavior of unfolded proteins.

CHAIN DYNAMICS OF UNFOLDED PROTEINS

The starting points for these investigations were proteins unfolded in aqueous solutions containing high concentrations of denaturants, such as urea or guanidinium chloride (GdmCl), which are a good solvent for unfolded proteins[54,82,83] and thus lead to protein unfolding. Under these conditions, noncovalent intrachain interactions are minimized and polypeptides are expected to approach the behavior of a homopolymer in good solvent. Correspondingly, unfolded proteins typically exhibit an expansion with increasing denaturant concentration.[15,39,73,84,85] nsFCS of the 66-residue cold shock protein (Csp) at 8M GdmCl revealed a reconfiguration time of 25 ± 5 ns (corrected for the change in solution viscosity caused by GdmCl),[40,47] which is remarkably fast and close to the dynamics expected for a simple Rouse or Zimm chain with the same dimensions. However, with decreasing denaturant concentration, the reconfiguration time, τ_r (corrected for solution viscosity), increased concomitantly with chain compaction, in contrast to the behavior expected from the Rouse or Zimm model, where chain compaction leads to a decrease in τ_r.[86] This discrepancy is an indication for the presence of internal friction, i.e., effects of interactions within the protein on chain dynamics. I will use the investigation of internal friction as an example to illustrate how single-molecule FRET combined with nsFCS can be employed to probe the behavior of unfolded proteins.

Internal friction had previously been investigated for folded proteins[87] and in the context of protein folding reactions,[88,89] where its molecular origin was mainly assigned to the large degree of desolvation in the very compact folded or transition states and the resulting decoupling from the solvent. For unfolded proteins, however, where the expansion of the chain relative to the folded state suggests pronounced solvation even in the absence of denaturants,[53,54] alternative concepts for quantifying the contribution of internal friction to protein dynamics and identifying its mechanistic origin had to be used. There is a long history of theoretical concepts in polymer dynamics that address the question of internal friction (or internal viscosity). Early ideas go back to the studies of Kuhn,[90] Cerf,[91] and de Gennes.[92] A particularly simple class of models that allow internal friction to be incorporated rigorously[93] are those of Rouse[94] and Zimm.[86,95] In the original Rouse theory,[94] chain dynamics are represented by the Brownian motion of coupled oscillators, i.e., beads representing individual chain segments connected by ideal springs whose dynamics are controlled only by the neighboring beads and the viscous drag from the solvent. Internal friction can be included in terms of an internal friction coefficient that impedes the relative motion of two beads.[96,97] Notably, this additional term does not change the eigenmodes of the system, but it increases all relaxation times by the same internal friction time, τ_i, yielding a spectrum of relaxation times, $\tau^{(n)} = \tau_{Rouse}/n^2 + \tau_i (n = 1, 2, \ldots)$, where τ_{Rouse} is the Rouse time, the largest relaxation time of

the Rouse chain without internal friction, and n is the mode number. A simple commonly used approximation is that only the dynamics corresponding to τ_{Rouse}/n^2 depend on solvent viscosity, η, whereas τ_i does not.[92] Since the overall solvent-dependent relaxation time, τ_s, with contributions from all relaxation modes, is the same as τ_{Rouse} to within a numerical factor,[98] we arrive at the relation $\tau_r = (\eta/\eta_0)\tau_s(\eta_0) + \tau_i$, where η_0 is the viscosity of water. If the chain reconfiguration time is measured as a function of solution viscosity and extrapolated linearly to zero viscosity, the internal friction time thus result as the intercept. Essentially the same behavior is found for the Zimm model when internal friction is included analogously, only with a mode dependence of $n^{-2/3}$ compared to n^{-2}.[93]

This behavior was observed by Soranno *et al.*[47] for unfolded Csp (Fig. 2). At 6M GdmCl, internal friction was negligible, but with decreasing denaturant concentration, τ_i increased to ~40 ns, much greater than τ_s under the same conditions, indicating the dominance of internal friction compared to solvent friction. An orthogonal approach to determine τ_i independent of changes in solution viscosity confirmed this result: Since the chain exhibits a spectrum of relaxation modes, each associated with a different length scale, segments of different lengths are affected by different parts of this spectrum,[98] and the relative contribution of internal friction to the reconfiguration dynamics will depend on the length of the segments.[97] By placing the FRET dyes in different positions within the chain, this signature becomes detectable: At low denaturant concentrations, τ_r is dominated by τ_i independent of segment length, whereas at high denaturant concentrations, the relaxation time scales with segment length as expected for a chain without internal friction [Fig. 2(b)]. Qualitatively similar behavior as for Csp was observed by Borgia *et al.* for the chemically unfolded spectrin domains R15 and R17.[99] However, in these cases, internal friction was detected even at the highest GdmCl concentrations, indicating a possible role of residual local interactions and secondary structure formation.

Rapid correlation experiments can be used to investigate not only chemically unfolded proteins but also proteins that are unfolded under physiological conditions. Interestingly, such IDPs typically exhibit global chain dynamics on similar time scales as chemically denatured proteins, in the range of ~10–100 ns,[30,47,100,101] and they also show internal friction.[30,47,100] An interesting trend is illustrated by a plot of τ_i versus the dimensions of the chains, which exhibits a decrease in τ_i with increasing chain expansion (Fig. 3), independent of whether this expansion is caused by the presence of denaturants or by the repulsion between charged residues in polyelectrolytic IDPs. Simple models of polymer dynamics, such as the Rouse or Zimm models with internal friction,[93] can thus provide a physically justified and self-consistent way of quantifying internal friction in unfolded and intrinsically disordered proteins. As recently shown by Hofmann and co-workers, a range of conceptually related models of polymer dynamics can be used to describe this experimentally observed behavior.[100] However, these models have a limited capacity for identifying the molecular origins of why the dynamics depend on solvent conditions or the degree of

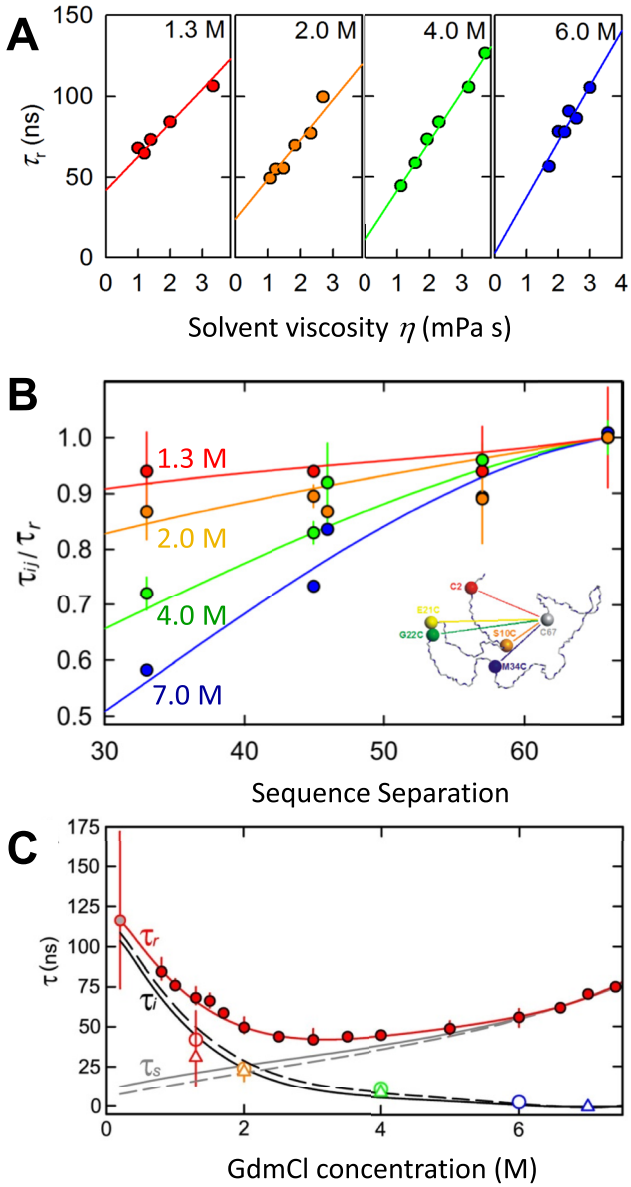

FIG. 2. Measuring internal friction in an unfolded protein. (a) Determining internal friction from the solvent viscosity dependences of chain reconfiguration times, τ_r, of terminally labeled Csp at different GdmCl concentrations (concentration indicated in the upper right of each panel). The data were fit with $\tau_r = (\eta/\eta_0)\tau_s(\eta_0) + \tau_i$ (solid lines) to extract the characteristic time scale associated with internal friction, τ_i. (b) Determining internal friction from the dependence of chain dynamics on the length of the polypeptide segment probed in unfolded Csp at different GdmCl concentrations (1.3M: red, 2.0M: orange, 4.0M: green, 7.0M: blue). The reconfiguration time, τ_{ij}, for the donor and acceptor in positions i and j normalized by the end-to-end reconfiguration time, τ_r, is shown as a function of the sequence separation, $|i - j|$. The fits with the Rouse model with internal friction used to determine the characteristic time scale associated with internal friction, τ_i, are shown as solid lines. (c) Quantifying internal friction as a function of denaturant concentration and comparison to (a) and (b). The experimentally determined GdmCl dependence of the end-to-end reconfiguration time, τ_r (filled red spheres), with an empirical polynomial fit used for interpolation (red line). The data point at the lowest GdmCl concentration was obtained in a microfluidic mixing experiment.[47] The solid (dashed) gray line shows the reconfiguration time expected for a Rouse (Zimm) chain in the absence of internal friction, τ_s. τ_i calculated for the Rouse and Zimm models is shown as solid and dashed black lines, respectively. The values of τ_i from this analysis agree well with the independently obtained values from (a) and (b) (shown as open circles and triangles, respectively), supporting the robustness of the analysis. Reproduced with permission from Soranno *et al.*, Proc. Natl. Acad. Sci. U. S. A. **109**(44), 17800–17806 (2012). Copyright 2012 National Academy of Sciences.

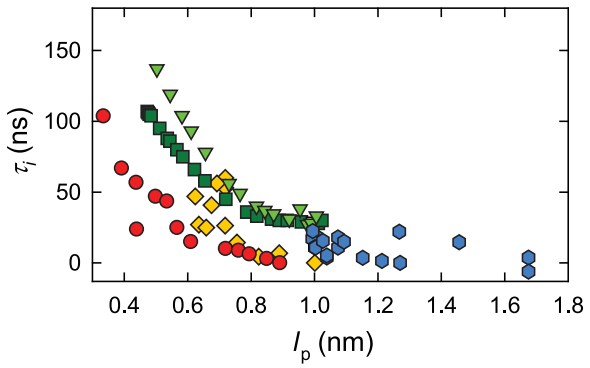

FIG. 3. Internal friction increases with increasing chain compaction. The dependence of the internal friction time, τ_i, on chain expansion for different unfolded proteins and IDPs, as indicated by their apparent persistence length, l_p, over a broad range of solution conditions shows a trend of more internal friction for more compact chains (prothymosin α, blue; the N-terminal domain of HIV integrase, yellow; Csp, red; spectrin R17, dark green; spectrin R15, light green).[47,99] Reprinted with permission from Schuler *et al.*, Annu. Rev. Biophys. **45**, 207–231 (2016). Copyright 2016 Annual Reviews.

compaction of the chain. A great opportunity for addressing such questions is the use of more detailed models in molecular simulations.

CLUES FROM MOLECULAR SIMULATIONS

Owing to the traditional focus on folded proteins in biology, force fields for molecular dynamics (MD) simulations were primarily optimized for proteins to form stable structures. As a result, the use of these potentials for unfolded or intrinsically disordered proteins typically yielded conformational ensembles that were much more structured and compact than observed experimentally. Triggered primarily by the increasing interest in IDPs, recent developments have changed this situation considerably.[7,11,12,102–106] Another important development has been the use of experimental restraints, where a simulated conformational ensemble is biased or reweighted based on experimental information, taking into account the uncertainties of the measurements.[85,107–109] These developments have started to enable a more and more realistic and detailed view of unfolded proteins.[102] Since the reconfiguration of unfolded proteins in the absence of persistent interactions occurs on the sub-microsecond time scale, MD simulations can now access these dynamics even in explicit solvent,[11,12,101,110,111] providing a new opportunity for identifying the molecular contributions affecting them. As an example, Fig. 4(a) illustrates the direct comparison of nsFCS data

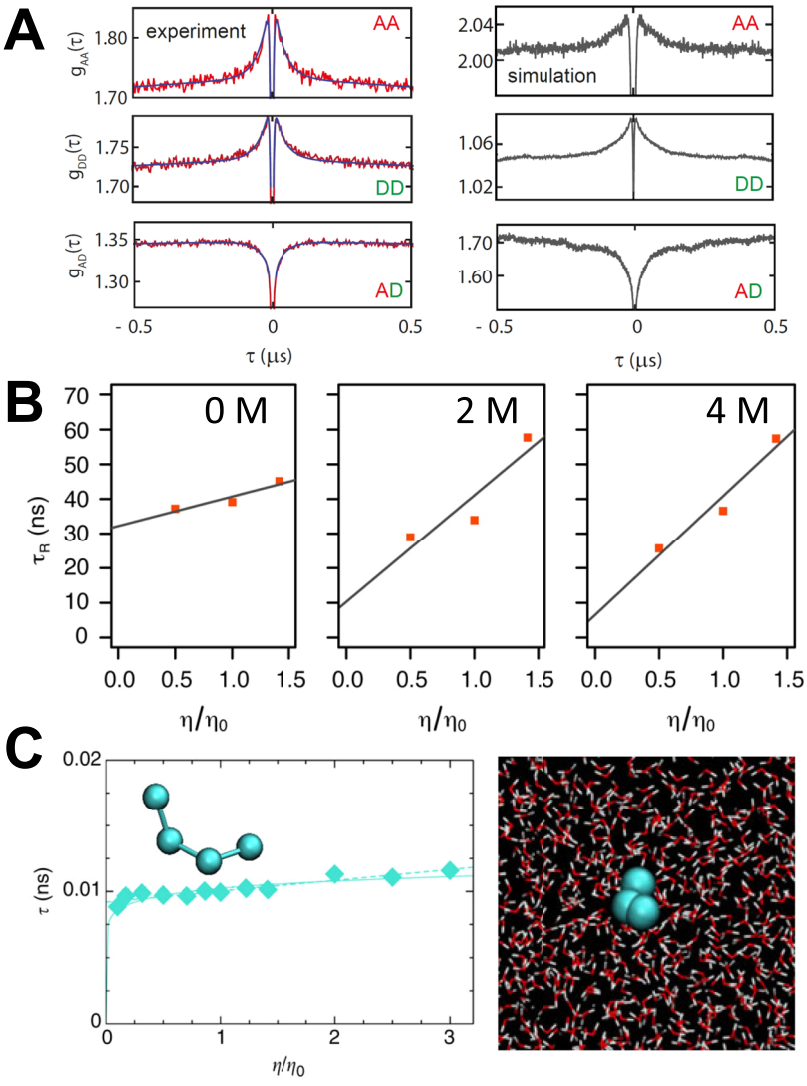

FIG. 4. Unfolded-state dynamics from molecular simulations. (a) Comparison of fluorescence correlation functions of unfolded state dynamics of protein L, observed experimentally (left) and calculated based on large-scale MD simulations (right), including the autocorrelation of acceptor fluorescence, $g_{AA}(\tau)$, donor fluorescence, $g_{DD}(\tau)$, and cross correlation of acceptor and donor fluorescence, $g_{AD}(\tau)$.[30] Experimental data[30] were taken at 3M GdmCl (black lines show a global fit of the three correlations with the reconfiguration time, τ_r, as a shared fit parameter), and MD simulations[12] were performed in the absence of denaturants. Adapted with permission from Soranno *et al.*, Proc. Natl. Acad. Sci. U. S. A. **114**(10), E1833–E1839 (2017). Copyright 2017 National Academy of Sciences. (b) Average end-to-end distance reconfiguration times (τ_R) as obtained from atomistic molecular dynamics simulations of unfolded Csp in explicit water plotted as a function of solvent viscosity at different GdmCl concentrations (as indicated in the upper right of the panels).[111] Note the similarity of the results to the experimental findings in Fig. 2(a). Adapted with permission from Echeverria *et al.*, J. Am. Chem. Soc. **136**(24), 8708–8713 (2014). Copyright 2014 American Chemical Society. [(c), left)] Viscosity dependence of the isomerization rate of a four-bead butane-like molecule used as a minimal model for dihedral transitions in water.[113] Each of the atoms has the Lennard-Jones parameters of an aliphatic carbon in the Amber ff03 force field. [(c), right)] Illustration of the molecule in explicit water. Adapted with permission from de Sancho *et al.*, Nat. Commun. **5**, 4307 (2014). Copyright 2014 Macmillan Publishers Ltd. In both simulations, solvent viscosity was varied by rescaling the masses of the water molecules.[117]

observed experimentally and calculated based on large-scale MD simulations of the same unfolded protein.[30]

To identify the origin of internal friction, Echeverria *et al.*[111] simulated unfolded Csp at different GdmCl concentrations and observed trends in remarkable agreement with the experimental data[47] [Fig. 4(b)]. Based on the analysis of the reconfiguration dynamics of the unfolded chain, the authors concluded that dihedral angle transitions provide the dominant mechanism of internal friction. Another potential contribution to the deviation of relaxation times in unfolded proteins from proportionality to solvent viscosity—the experimental signature ascribed to internal friction—is a low sensitivity of dihedral angle isomerization to solvent viscosity, which was predicted theoretically by Portman *et al.*[112] and identified to affect protein folding dynamics by de Sancho *et al.*[113] in simulations [Fig. 4(b)]. It appears that this effect is connected to memory friction introduced when a system crosses sharp local energy barriers on a time scale comparable to that of solvent relaxation.[114,115] Other possible contributions to internal friction come from non-native interactions, e.g., hydrogen bonds, as suggested by atomistic simulations of peptides.[116] A direct comparison of the dynamics of several unfolded proteins from large-scale MD simulations[12] with single-molecule fluorescence experiments indicated a greater abundance of transient non-native sequence-distant hydrogen bonds, salt bridges, and hydrophobic contacts in proteins that are more compact and exhibit more internal friction.[30] These increased interactions were correlated with slowed dihedral angle transitions, suggesting that the two contributions may be difficult to separate.

INTEGRATION OF METHODS

In view of such advances in methodology, we are thus at a very promising point for developing a much more complete understanding of the dynamics of unfolded and intrinsically disordered proteins. Single-molecule FRET combined with fluorescence correlation spectroscopy has opened a new window for probing global chain dynamics, but a comprehensive picture will require additional information from complementary techniques. Similar in spirit to the thriving field of integrative structural biology,[118] combining information from multiple sources will be essential for covering the entire range of relevant length scales and time scales, from the picosecond dynamics of the individual amino acid residue and nanosecond segmental dynamics to the sub-microsecond global chain dynamics and all the way to microsecond or even millisecond dynamics of IDPs comprising more persistent structures. Many spectroscopic techniques have the potential for providing pertinent additional information. Infrared spectroscopy is starting to resolve site-specific information down to picosecond times for larger proteins.[119] Neutron spin echo spectroscopy[120] may be the only other method besides nsFCS currently available for probing (bio)polymer chain dynamics in the tens of nanosecond range; it can reveal a large spectrum of relaxation modes and has been used to identify internal friction.[121,122] Arguably the most popular technique for IDPs is nuclear magnetic resonance (NMR) spectroscopy: While the time scales of global chain dynamics are difficult to access with NMR because of rotational decorrelation, the technique is ideal for obtaining a wealth of information on local dynamics, especially on the level of individual residues or segments forming secondary structures.[123,124] With such combined data acting as stringent benchmarks or restraints, it should ultimately be possible to use the framework of MD simulations to describe the complete structural and dynamic properties of unfolded and intrinsically disordered proteins from picoseconds to microseconds and beyond. At the same time, polymer theory and simple models will continue to be indispensable for identifying essential physical mechanisms and for the analysis of experimental data. The investigation of unfolded and intrinsically disordered proteins has thus become an inspiring arena for interdisciplinary research bringing together different experimental techniques with theory and simulation.

OPEN QUESTIONS AND CHALLENGES

With single-molecule spectroscopy and this growing repertoire of complementary methods, a range of open questions will become accessible. One direction will be to further probe effects of the solution conditions and the environment on the conformational ensembles and dynamics of unfolded proteins. The temperature dependence of chain dynamics[125] might offer further experimental clues as to the origin of internal friction, such as the presence of activated processes beyond solution viscosity; the role of charge regulation,[126] counterion condensation,[127] and charge renormalization[128] will be particularly important for a quantitative understanding of the structure and dynamics of highly charged IDPs; and the effects of macromolecular crowding,[129] i.e., the interactions with other macromolecules present in solution at a high concentration, might be particularly pronounced for unfolded and intrinsically disordered proteins with their weak intramolecular interactions and lack of well-defined three-dimensional structures.[49] The latter aspects provide a direct link to the cellular environment, where high concentrations of ions and biomolecules may modulate protein conformation and dynamics. The emerging possibility of single-molecule measurements in living cells[130] has started to enable a quantitative investigation of the dynamics of IDPs directly in their biological environment.[52]

A second direction of research will be to go beyond the behavior of individual polypeptide chains and develop a more quantitative understanding of the mechanisms involved in the many important interactions of IDPs with their cellular targets, be they other proteins, nucleic acids, lipids, small molecules, or metal ions. For these interactions, IDPs have been shown to employ a wide spectrum of mechanisms, where very different degrees of disorder can remain present in the bound state[4] so that the polymer aspects remain essential. While some IDPs fold upon binding,[3] many of them remain partially, largely, or even completely unstructured in the bound state.[131] In the extreme case, highly oppositely charged IDPs can interact with very high affinity and yet remain entirely unstructured in the complex[78] (Fig. 5). This type of behavior has been known for polyelectrolyte complexes of synthetic polymers[132,133] but had not been anticipated in biology. The closely related process of liquid-liquid phase separation or

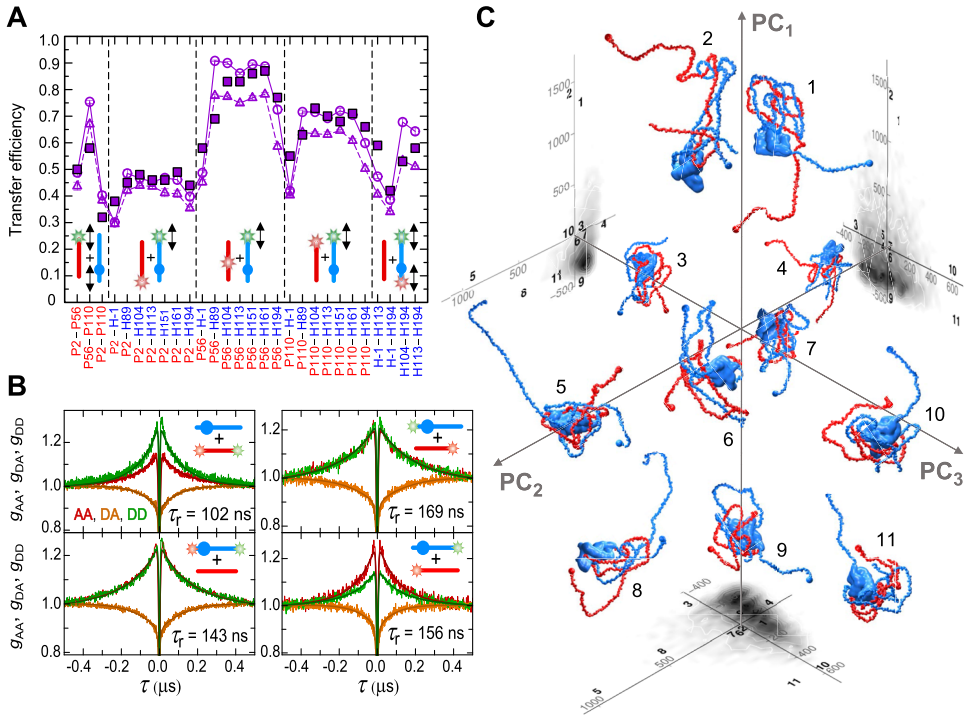

FIG. 5. Dynamics of two IDPs that bind with high affinity but remain disordered in the complex.[78] (a) Comparison of experimental (filled squares) and simulated transfer efficiencies (empty symbols) in the high-affinity complex between the two IDPs, histone H1 (H, blue pictogram) and prothymosin α (P, red pictogram), for the pairs of dye positions indicated below (triangles and circles: simulations with and without explicit chromophores, respectively). The results were used for parametrizing coarse-grained simulations of the complex, snapshots of which are shown in (c). (b) Examples of nsFCS probing long-range dynamics in the complex based on intra- and intermolecular FRET for the different dye positions illustrated in the pictograms of the two proteins. The resulting reconfiguration times, τ_r, are shown in each panel. (c) Examples of configurations of H (blue) and P (red) in the disordered complex based on coarse-grained simulations, illustrating the large range of arrangements. The structures are projected onto the first three principal components (PC) of the distance map, with projections of the full ensemble shown as gray scatter plots (units of Å). Numbers indicate the positions of the structures in the PC projections. Adapted with permission from Borgia *et al.*, Nature **555**(7694), 61–66 (2018). Copyright 2018 Macmillan Publishers Ltd.

coacervation[134] has recently enjoyed a remarkable revival in biology owing to its discovery as a mechanism of forming non-membrane bound compartments in cells.[135] Elucidating the structural and dynamic properties of disordered proteins in such multimolecular assemblies will be essential for bridging the gap between the molecular mechanisms[136] and the mesoscopic picture emerging from the concepts of phase separation.[135] Finally, understanding unfolded state dynamics may also be important for the pathological aggregation of proteins involved in many neurodegenerative diseases.[101,137] In summary, a vast array of questions related to the dynamics of unfolded and intrinsically disordered proteins is waiting to be addressed, and a wide range of methods and concepts from polymer physics, chemical physics, and soft matter physics will be essential for tackling these challenges. Single-molecule FRET combined with nsFCS has helped to open a new window into previously inaccessible length scales and time scales.

ACKNOWLEDGMENTS

I thank Alessandro Borgia, Robert Best, Hagen Hofmann, Dmitrii Makarov, Daniel Nettels, Andrea Soranno, and the members of my research group for stimulating discussions on over the years and for very helpful comments on the manuscript. This work was supported by the Swiss National Science Foundation.

[1] J. C. Kendrew, G. Bodo, H. M. Dintzis, R. G. Parrish, H. Wyckoff, and D. C. Phillips, Nature **181**(4610), 662–666 (1958).
[2] R. van der Lee, M. Buljan, B. Lang, R. J. Weatheritt, G. W. Daughdrill, A. K. Dunker, M. Fuxreiter, J. Gough, J. Gsponer, D. T. Jones, P. M. Kim, R. W. Kriwacki, C. J. Oldfield, R. V. Pappu, P. Tompa, V. N. Uversky, P. E. Wright, and M. M. Babu, Chem. Rev. **114**(13), 6589–6631 (2014).
[3] P. E. Wright and H. J. Dyson, Curr. Opin. Struct. Biol. **19**(1), 31–38 (2009).
[4] P. Tompa and M. Fuxreiter, Trends Biochem. Sci. **33**(1), 2–8 (2008).
[5] J. Habchi, P. Tompa, S. Longhi, and V. N. Uversky, Chem. Rev. **114**(13), 6561–6588 (2014).
[6] V. N. Uversky and A. K. Dunker, *Methods in Molecular Biology* (Springer, New York, 2012), Vol. 896.
[7] A. Vitalis and R. V. Pappu, J. Comput. Chem. **30**(5), 673–699 (2009).
[8] R. Wuttke, H. Hofmann, D. Nettels, M. B. Borgia, J. Mittal, R. B. Best, and B. Schuler, Proc. Natl. Acad. Sci. U. S. A. **111**(14), 5213–5218 (2014).
[9] R. B. Best and J. Mittal, J. Phys. Chem. B **114**(46), 14916–14923 (2010).
[10] P. S. Nerenberg, B. Jo, C. So, A. Tripathy, and T. Head-Gordon, J. Phys. Chem. B **116**(15), 4524–4534 (2012).
[11] R. B. Best, W. Zheng, and J. Mittal, J. Chem. Theory Comput. **10**(11), 5113–5124 (2014).
[12] S. Piana, A. G. Donchev, P. Robustelli, and D. E. Shaw, J. Phys. Chem. **119**(16), 5113–5123 (2015).
[13] K. A. Dill and D. Shortle, Annu. Rev. Biochem. **60**, 795–825 (1991).
[14] E. P. O'Brien, G. Morrison, B. R. Brooks, and D. Thirumalai, J. Phys. Chem. **130**(12), 124903 (2009).
[15] G. Ziv, D. Thirumalai, and G. Haran, Phys. Chem. Chem. Phys. **11**(1), 83–93 (2009).
[16] B. A. Shoemaker, J. J. Portman, and P. G. Wolynes, Proc. Natl. Acad. Sci. U. S. A. **97**(16), 8868–8873 (2000).

[17] A. S. Holehouse and R. V. Pappu, Annu. Rev. Biophys. **47**, 19 (2018).
[18] B. Schuler, H. Hofmann, A. Soranno, and D. Nettels, Annu. Rev. Biophys. **45**, 207–231 (2016).
[19] W. A. Eaton, Proc. Natl. Acad. Sci. U. S. A. **96**(11), 5897–5899 (1999).
[20] J. Sabelko, J. Ervin, and M. Gruebele, Proc. Natl. Acad. Sci. U. S. A. **96**(11), 6031–6036 (1999).
[21] J. Kubelka, J. Hofrichter, and W. A. Eaton, Curr. Opin. Struct. Biol. **14**(1), 76–88 (2004).
[22] O. Bieri, J. Wirz, B. Hellrung, M. Schutkowski, M. Drewello, and T. Kiefhaber, Proc. Natl. Acad. Sci. U. S. A. **96**(17), 9597–9601 (1999).
[23] L. J. Lapidus, W. A. Eaton, and J. Hofrichter, Proc. Natl. Acad. Sci. U. S. A. **97**(13), 7220–7225 (2000).
[24] H. Neuweiler, A. Schulz, M. Bohmer, J. Enderlein, and M. Sauer, J. Am. Chem. Soc. **125**(18), 5324–5330 (2003).
[25] K. Chattopadhyay, E. L. Elson, and C. Frieden, Proc. Natl. Acad. Sci. U. S. A. **102**(7), 2385–2389 (2005).
[26] S. Mukhopadhyay, R. Krishnan, E. A. Lemke, S. Lindquist, and A. A. Deniz, Proc. Natl. Acad. Sci. U. S. A. **104**(8), 2649–2654 (2007).
[27] A. Szabo, K. Schulten, and Z. Schulten, J. Chem. Phys. **72**(8), 4350–4357 (1980).
[28] L. J. Lapidus, P. J. Steinbach, W. A. Eaton, A. Szabo, and J. Hofrichter, J. Phys. Chem. B **106**(44), 11628–11640 (2002).
[29] A. Soranno, R. Longhi, T. Bellini, and M. Buscaglia, Biophys. J. **96**(4), 1515–1528 (2009).
[30] A. Soranno, A. Holla, F. Dingfelder, D. Nettels, D. E. Makarov, and B. Schuler, Proc. Natl. Acad. Sci. U. S. A. **114**(10), E1833–E1839 (2017).
[31] F. Zosel, D. Haenni, A. Soranno, D. Nettels, and B. Schuler, J. Chem. Phys. **147**(15), 152708 (2017).
[32] T. Förster, Ann. Phys. **437**(2), 55–75 (1948).
[33] B. W. Van Der Meer, G. Coker III, and S. Y. S. Chen, *Resonance Energy Transfer: Theory and Data* (VCH Publishers, Inc., New York, 1994).
[34] L. Stryer, Annu. Rev. Biochem. **47**, 819–846 (1978).
[35] T. Ha, T. Enderle, D. F. Ogletree, D. S. Chemla, P. R. Selvin, and S. Weiss, Proc. Natl. Acad. Sci. U. S. A. **93**(13), 6264–6268 (1996).
[36] A. A. Deniz, T. A. Laurence, M. Dahan, D. S. Chemla, P. G. Schultz, and S. Weiss, Annu. Rev. Phys. Chem. **52**, 233–253 (2001).
[37] Y. W. Jia, D. S. Talaga, W. L. Lau, H. S. M. Lu, W. F. DeGrado, and R. M. Hochstrasser, Chem. Phys. **247**(1), 69–83 (1999).
[38] A. A. Deniz, T. A. Laurence, G. S. Beligere, M. Dahan, A. B. Martin, D. S. Chemla, P. E. Dawson, P. G. Schultz, and S. Weiss, Proc. Natl. Acad. Sci. U. S. A. **97**(10), 5179–5184 (2000).
[39] B. Schuler, E. A. Lipman, and W. A. Eaton, Nature **419**(6908), 743–747 (2002).
[40] D. Nettels, I. V. Gopich, A. Hoffmann, and B. Schuler, Proc. Natl. Acad. Sci. U. S. A. **104**(8), 2655–2660 (2007).
[41] H. S. Chung, T. Cellmer, J. M. Louis, and W. A. Eaton, Chem. Phys. **422**, 229–237 (2013).
[42] I. V. Gopich and A. Szabo, Proc. Natl. Acad. Sci. U. S. A. **109**(20), 7747–7752 (2012).
[43] H. S. Chung, J. M. Louis, and I. V. Gopich, J. Phys. Chem. B **120**(4), 680–699 (2016).
[44] S. Kalinin, A. Valeri, M. Antonik, S. Felekyan, and C. A. Seidel, J. Phys. Chem. B **114**(23), 7983–7995 (2010).
[45] E. Sisamakis, A. Valeri, S. Kalinin, P. J. Rothwell, and C. A. M. Seidel, Methods Enzymol. **475**, 455–514 (2010).
[46] R. Ramanathan and V. Munoz, J. Phys. Chem. B **119**(25), 7944–7956 (2015).
[47] A. Soranno, B. Buchli, D. Nettels, R. R. Cheng, S. Müller-Späth, S. H. Pfeil, A. Hoffmann, E. A. Lipman, D. E. Makarov, and B. Schuler, Proc. Natl. Acad. Sci. U. S. A. **109**(44), 17800–17806 (2012).
[48] S. Müller-Späth, A. Soranno, V. Hirschfeld, H. Hofmann, S. Rüegger, L. Reymond, D. Nettels, and B. Schuler, Proc. Natl. Acad. Sci. U. S. A. **107**(33), 14609–14614 (2010).
[49] A. Soranno, I. Koenig, M. B. Borgia, H. Hofmann, F. Zosel, D. Nettels, and B. Schuler, Proc. Natl. Acad. Sci. U. S. A. **111**(13), 4874–4879 (2014).
[50] R. Kellner, H. Hofmann, A. Barducci, B. Wunderlich, D. Nettels, and B. Schuler, Proc. Natl. Acad. Sci. U. S. A. **111**(37), 13355–13360 (2014).
[51] H. Hofmann, F. Hillger, S. H. Pfeil, A. Hoffmann, D. Streich, D. Haenni, D. Nettels, E. A. Lipman, and B. Schuler, Proc. Natl. Acad. Sci. U. S. A. **107**(26), 11793–11798 (2010).
[52] I. Koenig, A. Zarrine-Afsar, M. Aznauryan, A. Soranno, B. Wunderlich, F. Dingfelder, J. C. Stüber, A. Plückthun, D. Nettels, and B. Schuler, Nat. Methods **12**(8), 773–779 (2015).
[53] A. Hoffmann, A. Kane, D. Nettels, D. E. Hertzog, P. Baumgärtel, J. Lengefeld, G. Reichardt, D. A. Horsley, R. Seckler, O. Bakajin, and B. Schuler, Proc. Natl. Acad. Sci. U. S. A. **104**(1), 105–110 (2007).
[54] H. Hofmann, A. Soranno, A. Borgia, K. Gast, D. Nettels, and B. Schuler, Proc. Natl. Acad. Sci. U. S. A. **109**(40), 16155–16160 (2012).
[55] M. Sauer, J. Hofkens, and J. Enderlein, *Handbook of Fluorescence Spectroscopy and Imaging: From Single Molecules to Ensembles* (Wiley-VCH, Weinheim, 2011).
[56] A. Grinvald, E. Haas, and I. Steinberg, Proc. Natl. Acad. Sci. U. S. A. **69**(8), 2273 (1972).
[57] I. V. Gopich and A. Szabo, in *Single-Molecule Biophysics: Experiment and Theory*, edited by T. Komatsuzaki, M. Kawakami, S. Takahashi, H. Yang, and R. J. Silbey (John Wiley & Sons, Inc., 2012), Vol. 146, pp. 245–297.
[58] B. Schuler, E. A. Lipman, P. J. Steinbach, M. Kumke, and W. A. Eaton, Proc. Natl. Acad. Sci. U. S. A. **102**, 2754–2759 (2005).
[59] W. Zheng, G. H. Zerze, A. Borgia, J. Mittal, B. Schuler, and R. B. Best, J. Chem. Phys. **148**(12), 123329 (2018).
[60] B. Schuler, J. Nanobiotechnol. **11**(Suppl. 1), S2 (2013).
[61] E. Haas, E. Katchalskikatzir, and I. Z. Steinberg, Biopolymers **17**(1), 11–31 (1978).
[62] D. Magde, W. W. Webb, and E. Elson, Phys. Rev. Lett. **29**(11), 705 (1972).
[63] M. Ehrenberg and R. Rigler, Chem. Phys. **4**(3), 390–401 (1974).
[64] E. Haas and I. Z. Steinberg, Biophys. J. **46**(4), 429–437 (1984).
[65] R. Hanbury Brown and R. Q. Twiss, Nature **177**(4497), 27–29 (1956).
[66] Ü. Mets, in *Fluorescence Correlation Spectroscopy*, edited by E. S. Elson and R. Rigler (Springer-Verlag, Berlin, 2001).
[67] A. J. Berglund, A. C. Doherty and H. Mabuchi, Phys. Rev. Lett. **89**(6), 068101 (2002).
[68] Z. S. Wang and D. E. Makarov, J. Phys. Chem. B **107**(23), 5617–5622 (2003).
[69] D. Nettels, A. Hoffmann, and B. Schuler, J. Phys. Chem. B **112**(19), 6137–6146 (2008).
[70] I. V. Gopich, D. Nettels, B. Schuler, and A. Szabo, J. Chem. Phys. **131**(9), 095102 (2009).
[71] P. R. Selvin and T. Ha, *Single-Molecule Techniques: A Laboratory Manual* (Cold Spring Harbor Laboratory Press, New York, 2008).
[72] X. Michalet, S. Weiss, and M. Jäger, Chem. Rev. **106**(5), 1785–1813 (2006).
[73] B. Schuler and H. Hofmann, Curr. Opin. Struct. Biol. **23**(1), 36–47 (2013).
[74] I. V. Gopich and A. Szabo, in *Theory and Evaluation of Single-Molecule Signals*, edited by E. Barkai, F. L. H. Brown, M. Orrit, and H. Yang (World Scientific Publishing Co., Singapore, 2009), pp. 1–64.
[75] E. Barkai, F. L. H. Brown, M. Orrit, and H. Yang, *Theory and Evaluation of Single-Molecule Signals* (World Scientific Publishing Co., Singapore, 2009).
[76] D. Nettels and B. Schuler, IEEE J. Sel. Top. Quantum Electron. **13**(4), 990–995 (2007).
[77] M. Aznauryan, L. Delgado, A. Soranno, D. Nettels, J. R. Huang, A. M. Labhardt, S. Grzesiek, and B. Schuler, Proc. Natl. Acad. Sci. U. S. A. **113**(37), E5389–E5398 (2016).
[78] A. Borgia, M. B. Borgia, K. Bugge, V. M. Kissling, P. O. Heidarsson, C. B. Fernandes, A. Sottini, A. Soranno, K. J. Buholzer, D. Nettels, B. B. Kragelund, R. B. Best, and B. Schuler, Nature **555**(7694), 61–66 (2018).
[79] V. A. Voelz, M. Jager, S. Yao, Y. Chen, L. Zhu, S. A. Waldauer, G. R. Bowman, M. Friedrichs, O. Bakajin, L. J. Lapidus, S. Weiss, and V. S. Pande, J. Am. Chem. Soc. **134**(30), 12565–12577 (2012).
[80] L. Fleury, J. M. Segura, G. Zumofen, B. Hecht, and U. P. Wild, Phys. Rev. Lett. **84**(6), 1148–1151 (2000).
[81] M. Brucale, B. Schuler, and B. Samori, Chem. Rev. **114**(6), 3281–3317 (2014).
[82] D. R. Robinson and W. P. Jencks, J. Biol. Chem. **238**, 1558–1560 (1963).
[83] J. E. Kohn, I. S. Millett, J. Jacob, B. Zagrovic, T. M. Dillon, N. Cingel, R. S. Dothager, S. Seifert, P. Thiyagarajan, T. R. Sosnick, M. Z. Hasan, V. S. Pande, I. Ruczinski, S. Doniach, and K. W. Plaxco, Proc. Natl. Acad. Sci. U. S. A. **101**(34), 12491–12496 (2004).
[84] G. Haran, Curr. Opin. Struct. Biol. **22**(1), 14–20 (2012).
[85] A. Borgia, W. Zheng, K. Buholzer, M. B. Borgia, A. Schuler, H. Hofmann, A. Soranno, D. Nettels, K. Gast, A. Grishaev, R. B. Best, and B. Schuler, J. Am. Chem. Soc. **138**(36), 11714–11726 (2016).
[86] M. Doi and S. F. Edwards, *The Theory of Polymer Dynamics* (Oxford University Press, USA, New York, 1988).

[87] A. Ansari, C. M. Jones, E. R. Henry, J. Hofrichter, and W. A. Eaton, Science **256**(5065), 1796–1798 (1992).
[88] S. J. Hagen, Curr. Protein Pept. Sci. **11**(5), 385–395 (2010).
[89] T. Cellmer, E. R. Henry, J. Hofrichter, and W. A. Eaton, Proc. Natl. Acad. Sci. U. S. A. **105**(47), 18320–18325 (2008).
[90] W. Kuhn and H. Kuhn, Helv. Chim. Acta **28**(7), 1533–1579 (1945).
[91] R. Cerf, J. Phys. Radium **19**(2), 122–134 (1958).
[92] P. G. De Gennes, *Scaling Concepts in Polymer Physics* (Cornell University Press, Ithaca, NY, 1979).
[93] R. R. Cheng, A. T. Hawk, and D. E. Makarov, J. Chem. Phys. **138**(7), 074112 (2013).
[94] P. E. Rouse, J. Chem. Phys. **21**(7), 1272–1280 (1953).
[95] B. H. Zimm, J. Chem. Phys. **24**(2), 269–278 (1956).
[96] E. R. Bazua and M. C. Williams, J. Chem. Phys. **59**(6), 2858–2868 (1973).
[97] B. S. Khatri and T. C. B. McLeish, Macromolecules **40**(18), 6770–6777 (2007).
[98] D. E. Makarov, J. Chem. Phys. **132**(3), 035104 (2010).
[99] A. Borgia, B. G. Wensley, A. Soranno, D. Nettels, M. Borgia, A. Hoffmann, S. H. Pfeil, E. A. Lipman, J. Clarke, and B. Schuler, Nat. Commun. **2**, 1195 (2012).
[100] A. Soranno, F. Zosel, and H. Hofmann, J. Chem. Phys. **148**(12), 123326 (2018).
[101] F. Meng, M. M. J. Bellaiche, J. Y. Kim, G. H. Zerze, R. B. Best, and H. S. Chung, Biophys. J. **114**(4), 870–884 (2018).
[102] R. B. Best, Curr. Opin. Struct. Biol. **42**, 147–154 (2017).
[103] W. Zheng, A. Borgia, M. B. Borgia, B. Schuler, and R. B. Best, J. Chem. Theory Comput. **11**(11), 5543–5553 (2015).
[104] E. P. O'Brien, G. Ziv, G. Haran, B. R. Brooks, and D. Thirumalai, Proc. Natl. Acad. Sci. U. S. A. **105**(36), 13403–13408 (2008).
[105] J. Huang, S. Rauscher, G. Nawrocki, T. Ran, M. Feig, B. L. de Groot, H. Grubmuller and A. D. MacKerell, Jr., Nat. Methods **14**(1), 71–73 (2017).
[106] P. Robustelli, S. Piana, and D. E. Shaw, Proc. Natl. Acad. Sci. U. S. A. **115**(21), E4758–E4766 (2018).
[107] G. Hummer and J. Kofinger, J. Chem. Phys. **143**(24), 243150 (2015).
[108] M. Bonomi, C. Camilloni, A. Cavalli, and M. Vendruscolo, Sci. Adv. **2**(1), e1501177 (2016).
[109] W. Boomsma, J. Ferkinghoff-Borg, and K. Lindorff-Larsen, PLoS Comput. Biol. **10**(2), e1003406 (2014).
[110] W. Zheng, A. Borgia, K. Buholzer, A. Grishaev, B. Schuler, and R. B. Best, J. Am. Chem. Soc. **138**(36), 11702–11713 (2016).
[111] I. Echeverria, D. E. Makarov, and G. A. Papoian, J. Am. Chem. Soc. **136**(24), 8708–8713 (2014).
[112] J. J. Portman, S. Takada, and P. G. Wolynes, J. Chem. Phys. **114**(11), 5082–5096 (2001).
[113] D. de Sancho, A. Sirur, and R. B. Best, Nat. Commun. **5**, 4307 (2014).
[114] R. F. Grote and J. T. Hynes, J. Chem. Phys. **73**(6), 2715–2732 (1980).
[115] G. S. Jas, W. A. Eaton, and J. Hofrichter, J. Phys. Chem. B **105**(1), 261–272 (2001).
[116] J. C. Schulz, L. Schmidt, R. B. Best, J. Dzubiella, and R. R. Netz, J. Am. Chem. Soc. **134**(14), 6273–6279 (2012).
[117] R. Walser and W. F. van Gunsteren, Proteins **42**(3), 414–421 (2001).
[118] A. B. Ward, A. Sali, and I. A. Wilson, Science **339**(6122), 913–915 (2013).
[119] K. L. Koziol, P. J. Johnson, B. Stucki-Buchli, S. A. Waldauer, and P. Hamm, Curr. Opin. Struct. Biol. **34**, 1–6 (2015).
[120] R. Biehl and D. Richter, J. Phys.: Condens. Matter **26**(50), 503103 (2014).
[121] A. M. Stadler, L. Stingaciu, A. Radulescu, O. Holderer, M. Monkenbusch, R. Biehl, and D. Richter, J. Am. Chem. Soc. **136**(19), 6987–6994 (2014).
[122] F. Ameseder, A. Radulescu, O. Holderer, P. Falus, D. Richter, and A. M. Stadler, J. Phys. Chem. Lett. **9**(10), 2469–2473 (2018).
[123] M. R. Jensen, R. W. Ruigrok, and M. Blackledge, Curr. Opin. Struct. Biol. **23**(3), 426–435 (2013).
[124] H. J. Dyson and P. E. Wright, Chem. Rev. **104**(8), 3607–3622 (2004).
[125] D. Nettels, S. Müller-Späth, F. Küster, H. Hofmann, D. Haenni, S. Rüegger, L. Reymond, A. Hoffmann, J. Kubelka, B. Heinz, K. Gast, R. B. Best, and B. Schuler, Proc. Natl. Acad. Sci. U. S. A. **106**(49), 20740–20745 (2009).
[126] M. Lund and B. Jonsson, Q. Rev. Biophys. **46**(3), 265–281 (2013).
[127] G. S. Manning and J. Ray, J. Biomol. Struct. Dyn. **16**(2), 461–476 (1998).
[128] W. Essafi, F. Lafuma, and C. E. Williams, Eur. Phys. J. B **9**(2), 261–266 (1999).
[129] H. X. Zhou, G. N. Rivas, and A. P. Minton, Annu. Rev. Biophys. **37**, 375–397 (2008).
[130] F. Persson, I. Barkefors, and J. Elf, Curr. Opin. Biotechnol. **24**(4), 737–744 (2013).
[131] T. Mittag, L. E. Kay, and J. D. Forman-Kay, J. Mol. Recognit. **23**(2), 105–116 (2010).
[132] A. F. Thünemann, M. Müller, H. Dautzenberg, J. F. O. Joanny, and H. Löwen, Adv. Polym. Sci. **166**, 113–171 (2004).
[133] V. A. Kabanov, Russ. Chem. Rev. **74**(1), 3–20 (2005).
[134] H. L. Bungenberg de Jong and W. J. Klaar, Trans. Faraday Soc. **28**, 27–68 (1932).
[135] A. A. Hyman, C. A. Weber, and F. Julicher, Annu. Rev. Cell Dev. Biol. **30**, 39–58 (2014).
[136] P. Li, S. Banjade, H. C. Cheng, S. Kim, B. Chen, L. Guo, M. Llaguno, J. V. Hollingsworth, D. S. King, S. F. Banani, P. S. Russo, Q. X. Jiang, B. T. Nixon, and M. K. Rosen, Nature **483**(7389), 336–340 (2012).
[137] L. J. Lapidus, Mol. Biosyst. **9**(1), 29–35 (2013).